Scaling up of the hybrid direct carbon fuel cell technology

CrossMark

Andrew C. Chien, Gale Corre, Rui Antunes, John T.S. Irvine*

School of Chemistry, University of St-Andrews, KY16 9ST, UK

ARTICLE INFO

ABSTRACT

A hybrid direct carbon fuel cell (HDCFC), combining molten carbonate fuel cell (MCFC) and solid oxide fuel cell (SOFC) technologies, is capable of converting solid carbon directly into electrical energy without intermediate reforming. The performance level achieved on small-scale cells (area <4 cm^2) suggests that engineering developments should now be undertaken to scale up and demonstrate the feasibility of practical systems. The scaling up of the HDCFC through the design and test of single stack repeat unit with realistic cell sizes was investigated in this study. A single cell of ~ 12.56 cm^2 active area produced a maximum power of ~ 1.2 W at 800 °C and a current density of ~ 200 mA cm^2 at 0.6 V, using wood-based pyrolyzed medium density fiberboard (p-MDF) as fuel. In comparison, the HDCFC with activated carbon as fuel produced a maximum power density of 36 and 53 mW cm^{-2} at 700 and 800 °C, respectively, and an electric efficiency of $\sim 40\%$ evaluated under 0.7 V for 17 h at 700 °C. These results demonstrated the applicability of HDCFC to practical systems while stack units were operated in batch mode and an appropriate fuel feeding mechanism has to be designed. Moreover, more engineering advances should be done to enhance power output since a HDCFC stack unit involves multiple challenges that have not been addressed yet, including system configuration and corrosion protection, and durability.

Copyright © 2012, Hydrogen Energy Publications, LLC. Published by Elsevier Ltd. All rights reserved.

1. Introduction

The reliance on carbonaceous solid fuels to fulfill our growing energy needs will remain significant in the near future. Coal is the main energy source in the world and its share of world energy consumption is bound to 27% in this decade [1]. Other solid carbon sources include petroleum coke, pyrolytic carbon, biomass, and municipal carbon waste such as medium density fiberboard (MDF). Among them, the MDF is produced from discarded household wooden furniture with more than 20 million cubic meters per year [2]. Hence, how to make good use of this resource should be investigated. Currently, the methods for converting solid carbon fuels to electricity suffer from low efficiencies due to thermodynamic limitations and heat loss in the current centralized electricity production system. Therefore, the development of technologies for converting carbon to electricity with improved efficiency and scalability is highly desirable.

The direct carbon fuel cell (DCFC) has gained significant interest to generate power from solid carbon electrochemically [3–7]. In principle, such fuel cells generate electricity with a thermodynamic efficiency nearly 100%, compared with 30–40% for the combustion process in coal-fired power plant. Furthermore, the fuel cells that separate oxidant (e.g. O^{2-} or CO_3^{2-}) and air allow to suppress NO_x production and can sequestrate the main product, CO_2, in a concentrated form for better air control. Other advantages such as scalability and quiet operation have a valuable diversity in stationary applications.

* Corresponding author. Tel.: +44 1334 463817; fax: +44 1334 463808.
E-mail addresses: jtsi@st-andrews.ac.uk, cyc2@st-andrews.ac.uk (J.T.S. Irvine).

Various concepts have since been proposed to develop DCFCs using molten salts [8—11] and solid oxide electrolytes [12—17]. The first type of DCFC was developed based on molten salt of alkali hydroxides, while the hydroxide is subject to degradation due to reaction with carbon dioxide. Replacement of hydroxide with carbonate salts overcomes the electrolyte degradation. Nevertheless, both hydroxide and carbonate molten salt corrode the components of fuel cell and pose difficult cell assembly. The solid electrolyte based DCFC provides the advantage of assembly and process simplicity. However, the performance of solid-electrolyte based DCFC (DC-SOFC) is limited because the contact for solid carbon, oxidant, and electronic conductor on the anode is confined. The OCVs obtained in DC-SOFCs differ from the theoretical value of carbon oxidation, i.e. 1.02 (volt), implying difficulties of direct oxidation [13,18—20].

Previous research in our group has focused on the development of hybrid direct carbon fuel cell (HDCFC) by combing advantages of molten salt and solid electrolyte fuel cells [18,21—23]. The HDCFC has a hybrid-state (molten and solid) electrode/electrolyte design, which increases the contact and cell performance by fluidity and mediation of molten salts [24—27] above solid electrolyte. As compared with molten carbonate fuel cells (MCFCs), the HDCFC avoids the CO_2 recirculation at the cathode; moreover, the introduction of the solid electrolyte protects the cathode from corrosion by the molten carbonates [4]. As compared to SOFCs, the introduction of the molten salt brings solid carbon to the interface of electrode/electrolyte, thus extending reaction zone from two-dimension to three-dimension and improving the cell performance.

Important advances in the HDCFC technology have previously been reported with pyrolyzed medium density fiberboard (PMDF) and activated carbon fuels using planar button cells made of NiO/YSZ/YSZ/LSM materials and a eutectic lithium/potassium molten carbonate. The power densities of 50 and 394 mW cm^{-2} were demonstrated using electrolyte-supported cells and anode supported cells, respectively, with open circuit voltages (OCV) of 1.15—1.23 V [18,23,28]. While research is still underway to improve performance and to better understand underlying reaction mechanisms as well as best operating conditions, the level of performance achieved in our previous results suggests that parallel developments should now be undertaken to demonstrate the feasibility of scaling up for practical HDCFC stacks.

Here, we demonstrate the HDCFC technology in a single cell with a large surface area as first step in the path from button cells to cell stacks. The design and the performance of a HDCFC stack repeat unit using commercially available solid oxide cells is presented. Such a unit will be subsequently repeated to build up the system for power output. We will show that the hybrid DCFC is, indeed, important in applying the upcoming direct carbon fuel technologies to coal conversion and achieving high performance for continuous power generation.

2. Experimental section

2.1. Cell assembly and current collection

A circular anode-supported cell (HC Starck) with a diameter of 50 mm was used in this study. The cell consists of a porous NiO/YSZ support layer (475—574 μm), a dense 8YSZ electrolyte (5—10 μm), a dense YDC layer (5—10 μm), and a LSCF perovskite material (30—50 μm). The NiO/YSZ layer is green with a diameter of 50 mm as an anode; the LSCF layer is black with a diameter of 40 mm as a cathode, shown in Fig. 1(a). Between the anode and cathode were sealed by one thermiculite ring gasket material (Thermiculite 866, Flexitallic) (I.D. = 50 mm, same as the cell size) to prevent gas from crossover as shown in Fig. 1(b).

The current collection was built with two strips of nickel mesh: one attached on the anode and the other attached on the cathode by silver paste. Two strips of nickel meshes were insulated by the previously mentioned thermiculite and fixed by another thermiculite ring (I.D. 40 mm, same as the cathode size) both on two electrodes, so short circuit can be avoided. The thermiculite material is chemically and thermally stable; in addition, the material is not degraded by the carbonates, thus allowing for efficient sealing and electrical insulation.

2.2. Cell testing and carbon/carbonate mixture

Fig. 2(a) shows the stack repeat unit for cell testing, consisting of an anode and cathode chamber made of stainless steel 316L. The cathode chamber features a gas flowing pattern machined onto the steel surface to allow for air flow. The anode chamber features a large cylindrical chamber that accommodates the carbon/carbonate mixture. The assembly of fuel cell with sealing and current collection was placed between two chambers, which was aligned and tightened by the screw through four holes machined throughout two chambers. The practical configuration after assemblage is depicted on Fig. 2(b).

The testing chamber was then placed in the furnace and heated to designed temperatures prior to performance
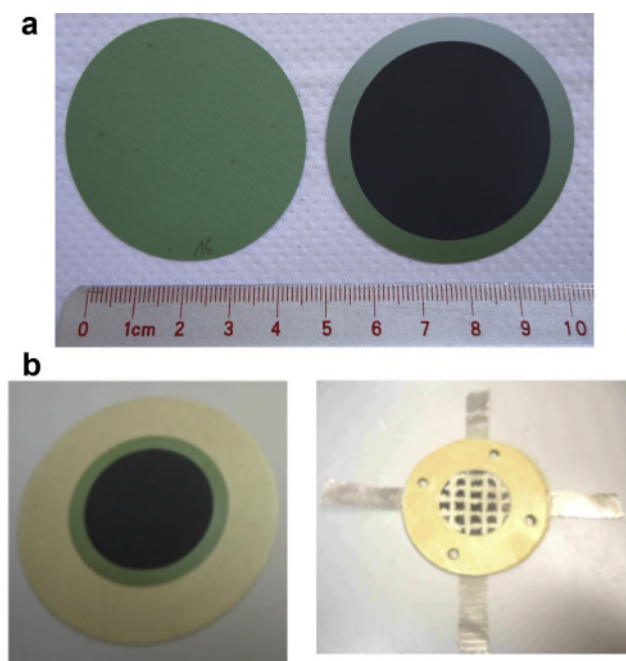

Fig. 1 — (a) An anode supported cell, (b) Seal with thermiculite and current collection.
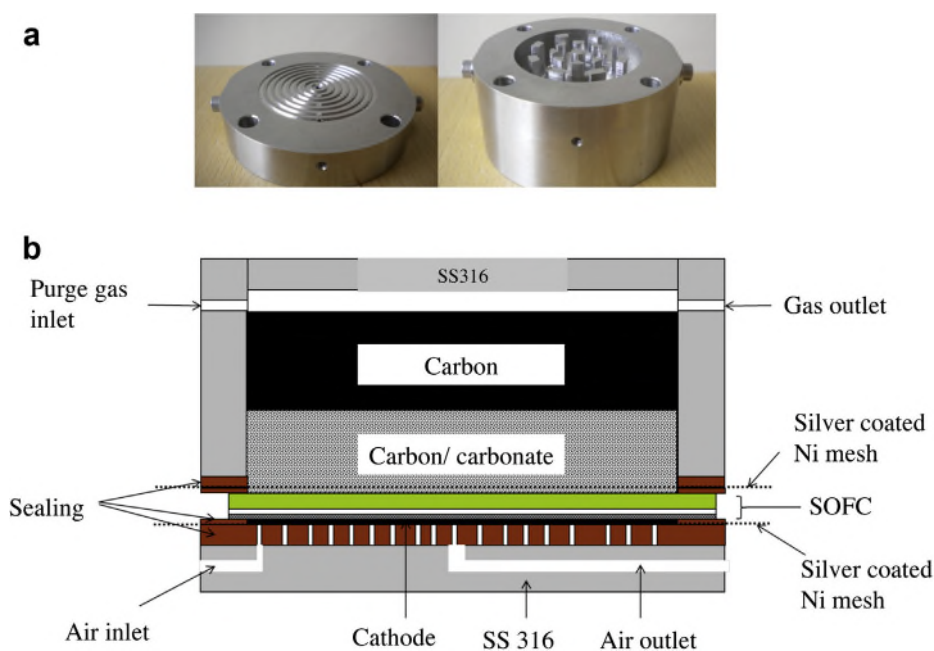
Fig. 2 — (a) Cathode chamber (left) and anode chamber (right), (b) The stack repeat unit for cell testing.

evaluation. For each temperature, a series of electrochemical measurements were taken after the cell was stabilized. The HDCFC was tested by passing N_2 on the anode and air on the cathode both with a flow rate of 50 cm^3 min^{-1}. On the other hand, the gas flow to anode was stopped in one experiment to investigate the effect on cell performance. The open circuit voltage (OCV), the cell voltage—current density characteristics (V—I curves) were measured and characterized by a Solartron potentiostat (Cell test system 1280 B). The long-term cell performance was evaluated by operating HDCFC under a load for a specific period of time.

Activated carbon (XC-72R, Cabot) and pyrolyzed medium density fiberboard (p-MDF, supplied by Marshall and Associates) were used as solid fuels. The molten salt used in the HDCFC is a lithium/potassium eutectic mixture prepared by physically mixing Li_2CO_3 (Aldrich) and K_2CO_3 (Fisher) powders in stoichiometric amounts (62/38 mol %). The weight ratio of carbon to carbonate was varied from 1 to 4 as specified.

3. Results and discussion

3.1. HDCFC performances with activated carbon fuels

Fig. 3 shows the power generation from an HDCFC with activated carbon as fuels operated under 0.7 V in batch mode at 700 °C. The power generation showed a parabolic profile with increasing power output in first 5 h, followed by a continuous decrease, indicating the behavior of operating in batch mode. As more power was generated, higher concentration of the oxidation product, i.e. CO and CO_2 were produced. The CO is a fuel that can be involved in electrochemical oxidation once CO is kept in the chamber. In addition, it was reasoned that the oxidation product, CO_2, has more residence time in a lower flow rate to react with solid carbon for CO, which in turn improve

power generation as shown in later (Fig. 5). The HDCFC reached a peak power density of 28 mW cm^{-2} and gave a total power of 4206 mW h (~15142 J) in 17 h consuming 1.5 g carbon fuels, compared with 15 mW cm^{-2} with electrolyte supported cells in same conditions [19]. The electric efficiency was determined to be 30—40%, depending on the heating value of carbon chosen (Pure carbon = 394 kJ mol^{-1}; coal = 300 kJ mol^{-1}, assuming CO_2 as a product).

$$\varepsilon_e = \frac{W_e}{\Delta H} = \frac{W_e}{(LHV)_c \cdot n_c} \cdot 100\%$$

ε_e: electric efficiency
W_e: electric work produced
$(LHV)_c$: low heat value of solid carbon
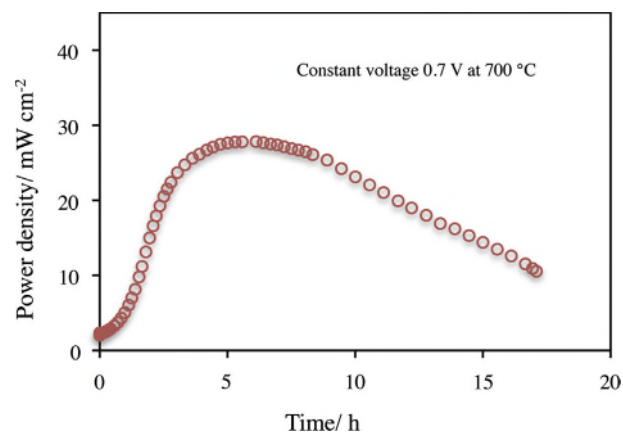n_c : mole of carbon consumed

Fig. 3 — Power vs. time profile of an HDCFC with 3 g of carbon (XC-72 R activated carbon)/carbonate mixture, weight ratio of carbon/carbonate = 1.
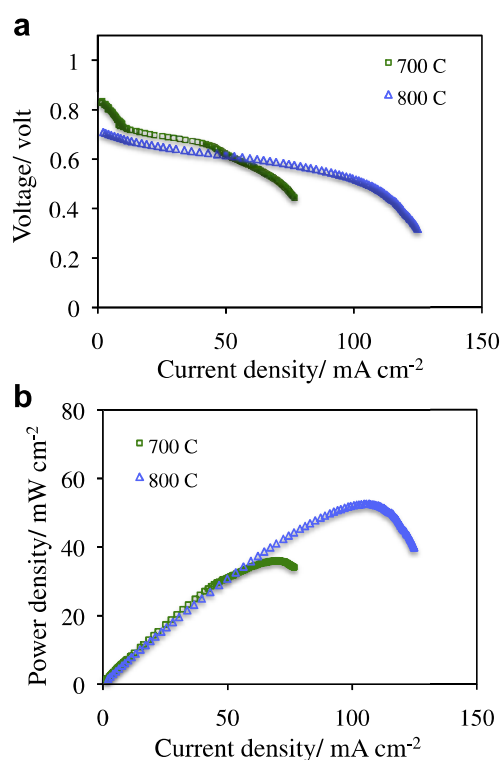
Fig. 4 — (a) V—I curve and (b) Power versus current curves of an HDCFC with 3 g mixture of carbon (XC-72 R activated carbon)/carbonate mixture (weight ratio of carbon/carbonate = 1) after 17 h under an electric load of 0.7 V.

The lower efficiency than a thermodynamic efficiency, ∼70% (operation at 0.7 V), could result from (i) incomplete fuel utilization due to escaping CO or air ingress, and (ii) loss from current collection. These losses can be avoided and improved by optimizing operation conditions such as gas flow and temperatures as well as choosing high conductive material that can withstand in corrosive environment for current collection.

Fig. 4 shows V—I and P—I curves of the HDCFC after 17 h under an electric load of 0.7 V at 700 and 800 °C. A maximum
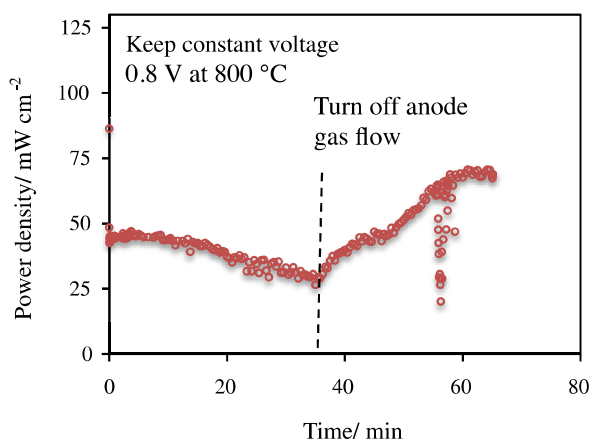

Fig. 5 — Power vs. time, with 6 g of carbon (p-MDF)/carbonate and nickel nitrate mixture, weight ratio of carbon/carbonate/nickel nitrate = 4/1/1.

power density of 36 and 53 m W cm^{-2} was obtained, respectively, at 700 and 800 °C. The V—I curves indicated that the cell was subject to concentration polarization at both temperatures, thereby limiting the cell performance. The concentration polarization was attributed to the depletion of carbon fuels in the anode chamber, which was inspected and it was found only a little carbon was left after cooling down. In addition, the HDCFC also showed a high electrode polarization at 700 °C, suggesting slow kinetics to initiate the carbon oxidation. Elevating temperature from 700 to 800 °C decreased the electrode polarization and improved the cell performance. Nevertheless, the OCV of HDCFC was close to the Ni—NiO redox potential, ∼0.7 (V), implying a shift of reaction mechanism and a high oxygen activity on the anode. The high oxygen activity further confirmed the diminishing carbon fuels and gas products, which could reduce NiO back to Ni.

$$C + O^{2-} \rightarrow CO + 2e^- \tag{1}$$

$$C \text{ or } CO + NiO \rightarrow CO_2 + Ni \tag{2}$$

$$Ni + O^{2-} \rightarrow NiO + 2e^- \tag{3}$$

3.2. HDCFC performance with p-MDF carbon fuel

Fig. 5 shows the power generation from a HDCFC with p-MDF as fuels operated under 0.8 V in batch mode at 800 °C. The power generation had an initial increase and then decreased continuously until the anode flow was stopped. Stopping the anode flow allows to utilize as much as possible the produced gas fuels from solid carbon, i.e. CO and H$_2$, as evidenced by the increased power generation. Compared with the activated carbon, the p-MDF seems to be more active in HDCFC with a much higher power output. In addition, the short initial increase in the HDCFC performance was indicative of little effect from gasification reactions since the activity of p-MDF is high enough and the reaction kinetics at 800 °C is fast. Nevertheless, the effect of added catalysts, i.e. nickel nitrate, have to be considered and need further studies.

Fig. 6 shows V—I and P—I curves of the HDCFC before and after 1 h under an electric load of 0.8 V at 800 °C. The straight V—I curves indicated that the major loss of HDCFC performance was from ohmic resistance. The obtained OCV was 0.99 V, closed to a theoretical value of carbon oxidation, i.e. 1.02 V. The maximum power output with and without anode gas flow was 69 and 92 mW cm^{-2}, respectively. These results not only confirmed the good adaptability of p-MDF to the HDCFC in our previous results [23,29] and presented the feasibility in engineering development on the HDCFC technology.

3.3. Reaction mechanisms

Owing to both oxygen anions (O^{2-}) and carbonate ion (CO$_3^{2-}$) as oxidants in the HDCFC, the actual anodic reactions are more complicated. Table 1 lists the detail of the anodic reactions in HDCFC consisting of MCFC and SOFC with carbonate and oxygen anions as separate oxidants. With carbonate as an oxidant, four major anodic reactions in MCFC, i.e. reactions (4)—(7), can be derived, depending on product distribution [30,31].
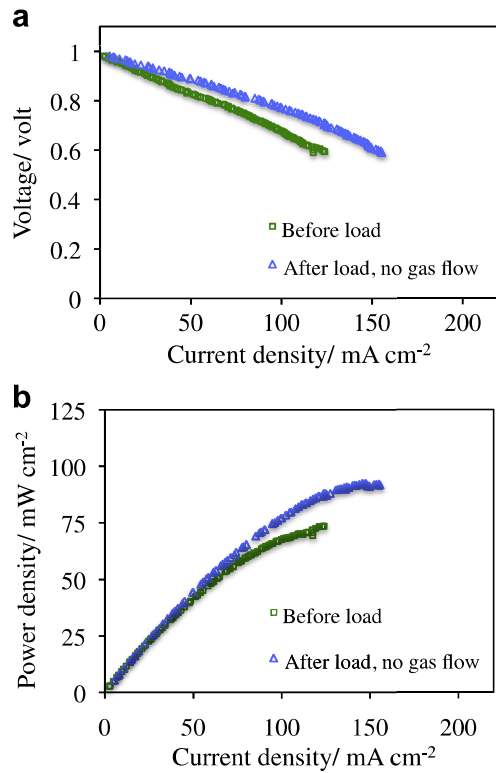
Fig. 6 — (a) V–I curve and (b) Power versus current curves of an HDCFC with 6 g of carbon (p-MDF)/carbonate/nickel nitrate mixture (weight ratio: 4/1/1) before and after an electric load of 0.8 V at 800 °C.
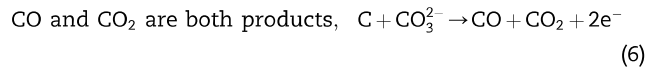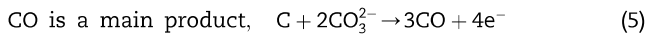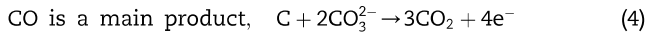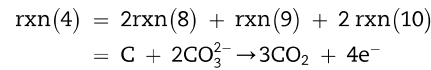
CO is a main product, $C + 2CO_3^{2-} \rightarrow 3CO_2 + 4e^-$ (4)

CO is a main product, $C + 2CO_3^{2-} \rightarrow 3CO + 4e^-$ (5)

CO and CO_2 are both products, $C + CO_3^{2-} \rightarrow CO + CO_2 + 2e^-$

(6)

CO oxidation is dominant, $CO + CO_3^{2-} \rightarrow 2CO_2 + 2e^-$ (7)

Table 1 — Detail reaction mechanisms in HDCFC.

Type	CO_3^{2-} oxidant	O^{2-} oxidant
MCFC	$C + 2CO_3^{2-} \rightarrow 3CO_2 + 4e^-$ (4)	$CO_3^{2-} \rightarrow CO_2 + O^{2-}$ (8)
		$C + CO_2 \rightarrow 2CO$ (9)
		$CO + O^{2-} \rightarrow CO_2 + 2e^-$ (10)
	$2C + CO_3^{2-} \rightarrow 3CO + 2e^-$ (5)	$CO_3^{2-} \rightarrow CO_2 + O^{2-}$ (8)
		$C + CO_2 \rightarrow 2CO$ (9)
		$C + O_2 \rightarrow CO + 2e^-$ (1)
	$C + CO_3^{2-} \rightarrow CO + CO_2 + 2e^-$	$CO_3^{2-} \rightarrow CO_2 + O^{2-}$ (8)
	(6) or simply sum of (4) and (5)	$C + O^{2-} \rightarrow CO + 2e^-$ (1)
	$CO + CO_3^{2-} \rightarrow 2CO_2 + 2e^-$ (7)	$CO_3^{2-} \rightarrow CO_2 + O^{2-}$ (8)
		$CO + O^{2-} \rightarrow CO_2 + 2e^-$ (10)
	–	$CO_3^{2-} \rightarrow CO_2 + O^{2-}$ (8)
		$2O^{2-} \rightarrow O_2 + 4e^-$ (11)
SOFC	–	$C + O_2 \rightarrow CO + 2e^-$ (1)
	–	$C + 2O^{2-} \rightarrow CO_2 + 4e^-$ (12)
	–	$CO + O^{2-} \rightarrow CO_2 + 2e^-$ (10)
	–	$2O^{2-} \rightarrow O_2 + 4e^-$ (11)

While these four reactions have been reported for direct carbon-MCFC (DC-MCFC), the direct oxidation of carbon by carbonate ion (CO_3^{2-}) is uncertain. On the other hand, carbonate ion may not be the basic oxidant unit. Decomposition of carbonate ion (CO_3^{2-}) is thermodynamically feasible in working conditions of MCFCs. Thus, O^{2-} generated from decomposition of CO_3^{2-} could be considered as the basic unit of oxidant. With O^{2-} as an oxidant, any of four major reactions in MCFC mentioned above can be grouped by the decomposition of carbonate with other side reactions such as reverse Boudouard reaction. For example, in reactions (4), CO_2 is a main product can be divided by:

$$CO_3^{2-} \rightarrow CO_2 + O^{2-}$$ (8)

$$C + CO_2 \rightarrow 2CO$$ (9)

$$CO + O^{2-} \rightarrow CO_2 + 2e^-$$ (10)

$$rxn(4) = 2\,rxn(8) + rxn(9) + 2\,rxn(10)$$
$$= C + 2CO_3^{2-} \rightarrow 3CO_2 + 4e^-$$

Furthermore, the O^{2-} could be also supplied from solid ionic conductor to molten salt. Indeed, this would enlarge the reaction zone in HDCFC and improve the cell performance.

4.   Conclusions

This study demonstrated the scaling-up of hybrid direct carbon fuel cell (HDCFC) technology with a commercial cell of large surface area housed in a robust stainless-steel testing chamber. The activated carbon and wood-based p-MDF was used as solid fuels for power generation. With activated carbon as fuels, a maximum power density of 36 and 53 mW cm^{-2} was obtained at 700 and 800 °C, respectively; an electric efficiency of operating under 0.7 V for 17 h was determined to be 30–40%. The lower efficiency than the theoretical value was attributed to incomplete fuel utilization and degrading current collection in corrosive environment. In comparison, the HDCFC with p-MDF as fuels produced a maximum power of 92 mW cm^{-2} at 800 °C without anode gas flow. Stopping the anode flow allowed that fuel utilization could be complete as much as possible, thus increasing power generation. The wood-based p-MDF showed a high activity and good adaptability in the HDCFC, which is promising for employing abundant municipal solid carbon waste to generate electricity.

Designing a HDCFC stack unit involves multiple challenges that have not been addressed yet, including system configuration, corrosion protection, current collection or sealing. As HDCFCs involve solid fuels, a major challenge in the development of practical systems will be the design of an appropriate fuel feeding mechanism. While this issue was not addressed in the present study and stack units were operated in batch mode, the work of continuous feeding is on going.

Acknowledgments

REFERENCES

[1] International Energy Outlook 2009 and http://www.eia.doe.gov/oiaf/ieo/coal.html.
[2] Wood Panel Industries Federation website website http://www.wpif.org.uk/publications/PressRelease-MDF.pdf.
[3] Cao D, Sun Y, Wang G. J Power Sources 2007;167:250—7.
[4] Gür TM. J Electrochem Soc 2010;157:B751—9.
[5] Rady AC, Giddey S, Badwal SPS, Ladewig BP, Bhattacharya S. Energy Fuels 2012;26:1471—88.
[6] Giddey S, Badwal SPS, Kulkarni A, Munnings C. Prog Energ Combust 2012;38:360—99.
[7] Cinti G, Hemmes K. Int J Hydrogen Energy 2011;36:10198.
[8] Zecevic S, Patton EM, Parhami P. Carbon 2004;42:1983—93.
[9] Cherepy NJ, Krueger R, Fiet KJ, Jankowski AF, Cooper JF. J Electrochem Soc 2005;152:A80—7.
[10] Li X, Zhu Z, Marco RD, Bradley J, Dicks AJ. Phys Chem A 2010; 114:3855—62.
[11] Chen M, Wang C, Niu X, Zhao S, Tang J, Zhu B. Nt J Hydrogen Energy 2010;35:2732—6.
[12] Li S, Lee AC, Mitchell RE, Gür TM. Solid State Ionics 2008;179: 1549—52.
[13] Chien AC, Chaung SSC. J Power Sources 2011;196:4719—23.
[14] Nürnberger S, Bußar R, Desclaux PN, Franke B, Rzepka M, Stimming U. Energy Environ Sci 2010;3:150—3.
[15] Desclaux P, Nürnberger S, Rzepka M, Stimming U. Int J Hydrogen Energy 2011;36:10278—81.
[16] Tang YB, Liu J. Int J Hydrogen Energy 2011;35:11188.
[17] Bai YH, Liu Y, Tang YB, Xie YM, Liu J. Int J Hydrogen Energy 2011;36:9189.
[18] Nabae Y, Pointon KD, Irvine JTS. Energy Environ Sci 2008;1: 148—55.
[19] Jiang C, Irvine JTS. J Power Sources 2011;196:7318—22.
[20] Chien AC, Siengchum T, Chuang SSC. ECS Trans 2011;33: 75—85.
[21] Pointon KD, Irvine JTS, Lakeman B, Bradley J, Jain SJ. Power Source 2006;162:750—6.
[22] Nabae Y, Pointon KD, Irvine JTS. J Electrochem Soc 2009;156: B716—20.
[23] Jiang C, Ma J, Bonaccorso AD, Irvine JTS. Energy Environ Sci 2012;5:6973—80.
[24] Jain SL, Nabae Y, Lakeman BJ, Pointon KD, Irvine JTS. Solid State Ionics 2008;179:1417—21.
[25] Xia C, Li Y, Tian Y, Liu QH, Zhao YC, Jia LJ, et al. Power Sources 2009;188:156—62.
[26] Peelen WHA, Hemmes K, D.W. JHW. High Temp Mater Process 1998;2:471.
[27] Hemmes K. In: White RE, Vayenas, editors. Modern aspects of Electrochemistry, vol. 37. Kluwer Academic/Plenum Publishers; 2004. p. 131.
[28] Hemmes K, Cassir M. J Fuel Cell Sci Technol 2011;8: 051005.
[29] Jain SL, Lakeman JB, Pointon KD, Marshallc R, Irvine JTS. Energy Environ Sci 2009;2:687—93.
[30] Hemmes K, Peelen WHA, de Wit JHW. Electrochim Acta 1998; 43(14—15):2025—31.
[31] Peelen WHA, van Driel M, Hemmes K. Electrochim Acta 1998; 43:3313—31.